Use of ATOVS raw radiances in the operational assimilation system at Météo-France

Élisabeth Gérard, Florence Rabier, Delphine Lacroix
Météo-France, Toulouse, France
Zahra Sahlaoui
Maroc-Météo, Casablanca, Morocco

Introduction

To set up the technical context, it should be reminded that Météo-France system shares the code with ECMWF and benefits from the developments in satellite data assimilation. Since 22 October 2002 Météo-France has been using ATOVS raw radiances instead of preprocessed radiances in operations. This migration was intended to be conducted in three steps: the assimilation of (1) AMSU A data – which became operational on 22 October 2002 -, then (2) HIRS data – which became operational on 8 December 2003 - and finally (3) AMSU B data – in research mode -. This strategy is motivated by the fact that assimilating infrared data requires a reliable cloud detection technique and assimilating humidity sensitive radiances comes naturally after assimilating temperature sensitive radiances. The experiments were performed on the stretched spectral global model ARPEGE with 43 hybrid coordinate vertical levels from the surface up to about 1 hPa. An horizontal thinning is performed to ensure a minimum distance of about 250 km between raw radiances (as for preprocessed radiances). Bias correction coefficients are computed following Harris and Kelly (2001). A succession of assimilation cycles performed with the data whose impact is to be evaluated will be called “Experiment” and a succession of cycles without these new features will be called “Control”.

Assimilation of AMSU A raw radiances

NESDIS preprocessed data undergo significant preprocessing consisting mainly in instrument collocation and creation of cloud flags. Complicated random and systematic errors are introduced by this process in the data and a direct use of raw radiances can indeed bypass this problem. In doing this, the 1DVar scheme used jointly with the preprocessed data in the assimilation is not used anymore, so that two specific actions have to be performed (Gérard et al. 2002): (1) the lower and upper bounds of the RTTOV-7 radiative transfer model, which requires the vertical temperature profile on 43 pressure levels from 1013.25 hPa up to 0.1 hPa, are controlled by respectively introducing model surface temperature into the control variable and extrapolating the model temperature profile from the top of the atmospheric model (1 hPa) to the top of the radiative transfer model (0.1 hPa) by a regression (Clément Chouinard, personal communication); (2) as the 1DVar cloud flag is not available anymore, rain contaminated data, that hinder from using AMSU A rain sensitive lowest channels, are detected with a test on AMSUA window channel 4 observation departure from first guess. The threshold set to 1.5 K when implementing in operations the assimilation of AMSU A raw radiances has been revisited since then and re-evaluated to

0.7 K for more drastic control of the rain contaminated data (as done at ECMWF**)** and completed by a threshold of 0.1 mm on cloud liquid water path derived from AMSU A channels 1 and 2. Details on the conditions of use of each channel are listed in Table 1, showing special caution for using low peaking channels over land, over sea ice and in cloudy conditions.

Table 1: Conditions of use of AMSU A channels. Each condition is necessary but not sufficient. T_s is the model surface temperature, orog is the model altitude, obs-fg is the observation departure from first guess, ch stands for channel and lat for latitude. Blue ✓ refers to specific sub-conditions.

Conditions of use ✓	**1**	**2**	**3**	**4**	**5**	**6**	**7**	**8**	**9**	**10**	**11**	**12**	**13**	**14**	**15**
3 < scan position < 28					✓	✓	✓	✓	✓	✓	✓	✓			
Open sea (T_s > 271.45 K)					✓	✓	✓	✓	✓	✓	✓	✓			
Sea ice ($T_s \leq$ 271.45 K)							✓	✓	✓	✓	✓	✓			
Land orog < 500/1500 m for channels 5/6					✓	✓	✓	✓	✓	✓	✓	✓			
Clear $\lvert$obs-fg$\rvert_{ch\,4} \leq$ 1.5 K					✓	✓	✓	✓	✓	✓	✓	✓			
Cloudy $\lvert$obs-fg$\rvert_{ch\,4}$ > 1.5 K $\lvert$lat$\rvert$ > 30° for channel 8								✓	✓	✓	✓	✓			

The assimilation of AMSU A raw radiances was found to behave better than the assimilation of AMSU A and HIRS preprocessed radiances on a one month pre-operational suite in Aug-Sep 2002, especially in the Southern Hemisphere, in the upper troposphere and in the short forecast range, as illustrated by the 200 hPa geopotential height performance at day 1 in Fig. 1. On a global scale AMSU A raw radiances enable the 200 hPa geopotential height forecast root mean square (rms) error to be reduced by about 1 m in the Northern Hemisphere and about 3 m in the Southern Hemisphere, despite the loss of HIRS data. However the lack of HIRS humidity information was felt, especially in the tropical regions; reintroducing HIRS data in the operational assimilation turned out to be a priority.

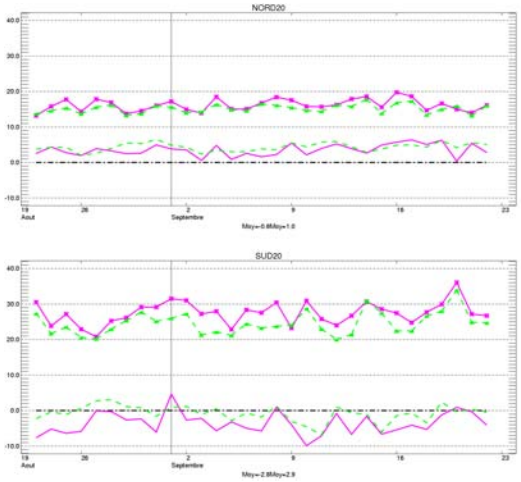

Fig. 1: Time series (22 Aug – 22 Sep 2002) of rms error (curves with symbols) and bias (curves without symbol) for 24 hour forecast of 200 hPa geopotential height when compared to each experiment's own analysis, in the Northern Hemisphere (top) and the Southern Hemisphere (bottom). Control (with preprocessed AMSU A and HIRS data) in pink, Experiment (with AMSUA raw radiances) in green.

Assimilation of HIRS raw radiances

The problem of using HIRS data is to efficiently detect cloud effects in the measured signal. As done for detecting AMSU A rain contaminated data, cloud detection is performed through a test on HIRS observation departure from the first guess in a window channel, i.e. HIRS channel 8 is selected for this task. As done at ECMWF, and with the same thresholds, this test is asymmetric, depends on channel and latitude band. Moreover, as this departure is influenced by surface temperature, sea ice situations are rejected in order not to contaminate this test by erroneous surface temperatures, as shown in Table 2.

Table 2: Conditions of use of HIRS channels. Each condition is necessary but not sufficient. T_s is the model surface temperature, orog is the model altitude, obs-fg is the observation departure from first guess, ch stands for channel and lat for latitude. Blue columns are associated to HIRS water vapour channels. For last row see Text.

Conditions of use ✓	**1**	**2**	**3**	**4**	**5**	**6**	**7**	**8**	**10**	**11**	**12**	**13**	**14**	**15**
3 < scan position < 54				✓	✓	✓	✓			✓	✓		✓	✓
Open sea (T_s > 271.45 K)				✓	✓	✓	✓			✓	✓		✓	✓
Land (orog < 1500 m)											✓			
Clear:														
↳ x(ch,lat) < (obs-fg) $_{ch\ 8}$ ≤ y(ch,lat)				✓	✓	✓	✓			✓	✓		✓	✓
↳ (obs-fg) $_{ch\ 11/12}$ > -3 K										✓	✓			

Research experiments proved to be beneficial to both analysis and forecast performances. However, an unexpected problem showed up in the pre-operational suite which turned out to be unhealthy after a few analysis days, as analysis temperature field was characterised by a succession of large increases and large decreases along the vertical in the upper model levels in the polar regions of the Northern Hemisphere (what is called a “ringing problem”). This problem is probably linked to particular meteorological conditions. The left panel of Fig. 2 illustrates the large temperature decrease at the top of the model, down to about –35 K locally, and about –11 K on average over two weeks in the 60°N-90°N latitude band. These large increments were associated to misused data in undetected cloudy regions, in areas sparsely covered by other observations that might constrain the model backwards, once damage has been done. The guilty observations were found to be water vapour channels 11 and 12 observations, which appeared not to be properly selected: despite the blacklisting and the first guess quality control (see an example of data selection on Fig. 3), some data with largely negative departures from first guess in these channels, i.e. cloud contaminated data, are used in the assimilation, and this bad effect is transported upwards to higher model levels through the background error covariance matrix. Conditions were added on observation departure from first guess in channels 11 and 12, so that any observation characterised by a departure lower than –3 K in these channels is rejected (as indicated in the last row of Table 2 and with red dotted lines on Fig. 3). These conditions appeared to be sufficient to solve the ringing problem, as shown on the right panel of Fig. 2. On average over two weeks in the 60°N-90°N latitude band, temperature analysis differences in absolute value are lower than 0.2 K when the new HIRS blacklist is applied.

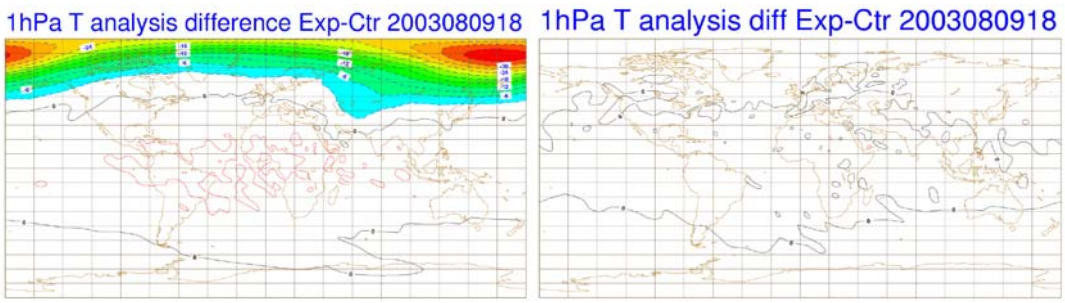

Fig. 2: 1hPa temperature analysis difference between the Experiment (with HIRS data) and the Control (without HIRS data) on 9th Aug 2003 at 18 UTC, 9 days after the beginning of the assimilation period, on the left with the initial blacklist, on the right with the new blacklist (as presented in Table 2). Contour interval is 3 K on both plots.

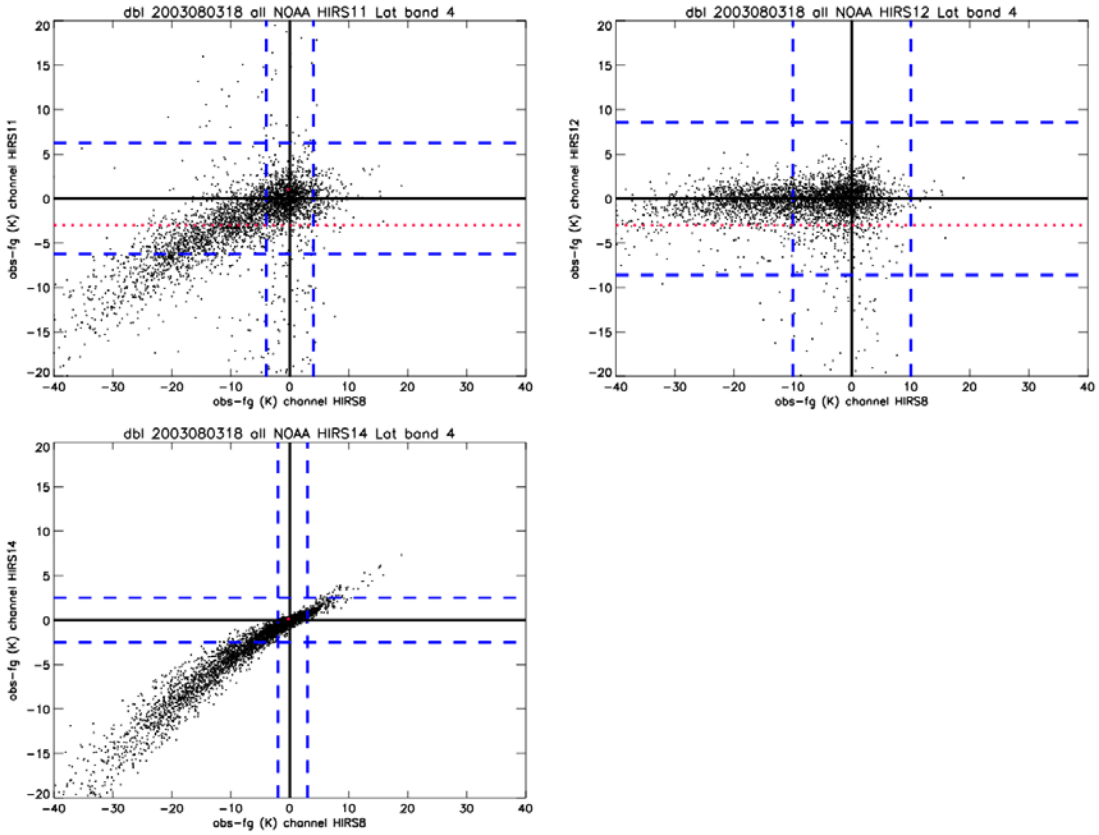

Fig. 3: An example of data selection on quality criteria (no thinning is performed on this particular dataset) for HIRS channels 11 (upper left), 12 (upper right) and 14 (lower left) in the 60°N-90°N latitude band. Thresholds for cloud detection as associated to HIRS channel 8 observation departure from first guess are represented by straight blue lines parallel to the y-axes; first guess quality control thresholds are represented by straight blue lines parallel to the x-axes. Straight red dotted lines represent the additional threshold on channel 11 and 12 observation departures from first guess. A few red isolated dots correspond to data rejected by the CO_2 slicing cloud detection/position method (Kelly, 2003).

Winter (25 Dec 2002 – 11 Jan 2003) and summer (1-17 Aug 2003) experiments were re-run with the new HIRS blacklist. The time series of total column water vapour (TCWV) over the global area are given in Fig. 4 for both periods and statistics on the change in TCWV related to the use of HIRS data are provided for different areas in Table 3. For both periods a global drying of the atmosphere is noticeable, the Experiment analysis has globally 4% (summer) to 6% (winter) less water vapour than the Control analysis; this feature seems to be realistic, as confirmed by the ECMWF analysis (not shown). The biggest relative TCWV decrease is found in the Tropics followed by the Southern Hemisphere. However a slight moistening can also occur in the Northern Hemisphere, over land in winter and over sea in summer.

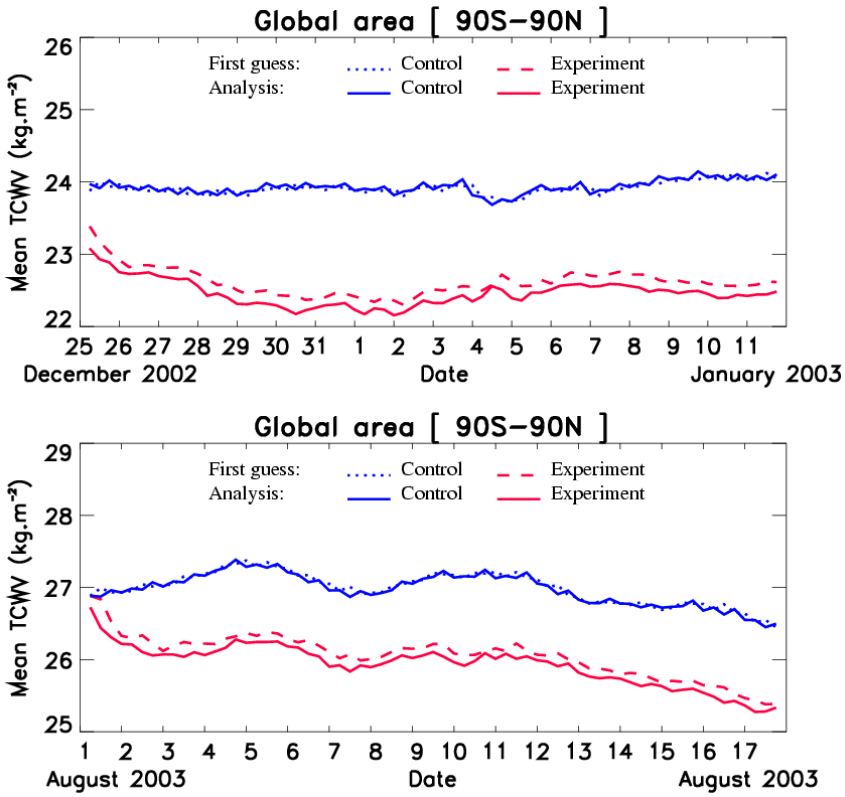

Fig. 4: Time series of total column water vapour (TCWV) globally derived from the first guess and analysis for the Control (without HIRS) and the Experiment (with HIRS) over the winter period (top panel) and the summer period (bottom panel).

Table 3: Relative total column water vapour (TCWV) change obtained in the analysis when using HIRS data, expressed in percent of TCWV obtained without using HIRS data, for the winter (left) and summer (right) periods, for different latitude bands and as a function of the landsea mask.

	WINTER				SUMMER		
%	Global	Sea	Land	%	Global	Sea	Land
Globe	-6.1	-7.4	-0.1	Globe	-3.9	-5.1	-0.3
N. Hem	-3.0	-4.3	0.8	N. Hem	1.1	1.9	-0.1
Tropics	-8.0	-9.6	-0.6	Tropics	-7.1	-8.7	-0.7
S. Hem	-4.7	-3.2	0.5	S. Hem	-3.3	-3.7	0.7

On average over the summer period the relative minimum, that characterizes the vertical profile of specific humidity analysis difference between Experiment and Control, is in the vicinity of 800 hPa as shown in Fig. 5 (top panel),as is the vertical profile of specific humidity increment (analysis minus first guess)in the Experiment (bottom panel). Results for the winter period are similar (not shown). The increments are globally negative throughout the Experiments. The negative TCWV increments should decrease during the Experiments if the assimilation and short-range forecast processes were optimal. However, the constant need to remove moisture at each assimilation cycle (see Fig. 4), especially in the Tropics, reveals that the system produces “undesired” moisture during the following six hours.

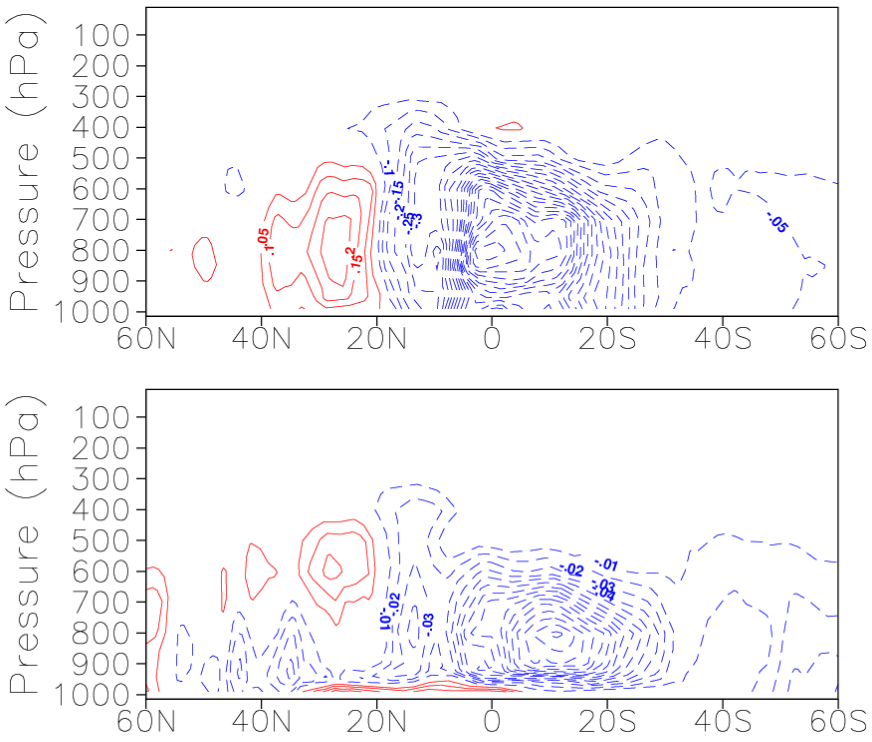

Fig. 5: Zonal mean of specific humidity analysis difference between the Experiment and the Control (top panel) and Experiment increments – analysis minus first guess -(bottom panel), averaged over the summer period and over longitude. The x-axes represent the latitude. The contour interval is 0.05 g.kg^{-1} (top panel) and 0.01 g.kg^{-1} (bottom panel), with solid red contours representing a moistening (positive values) and dashed blue ones a drying (negative values) in the analysis, when compared to Control analysis (top panel) and Experiment first guess (bottom panel).

Despite the disturbed hydrological cycle of the model, HIRS data help to improve the forecast performances, as illustrated by the reduction of rms error of day 2 forecast of geopotential height at 500 hPa to about 1.1 m in the Northern Hemisphere and 1.4 m in the Tropics and Southern Hemisphere during the winter period (Fig. 6). Another illustration of the beneficial effect of HIRS data can be found during the summer period over Europe and North Atlantic Ocean for example (Fig. 7), where medium range forecast performances at day 3 and day 4 are improved (bias and rms error reduction) for geopotential height, wind and relative humidity especially in the mid and upper troposphere.

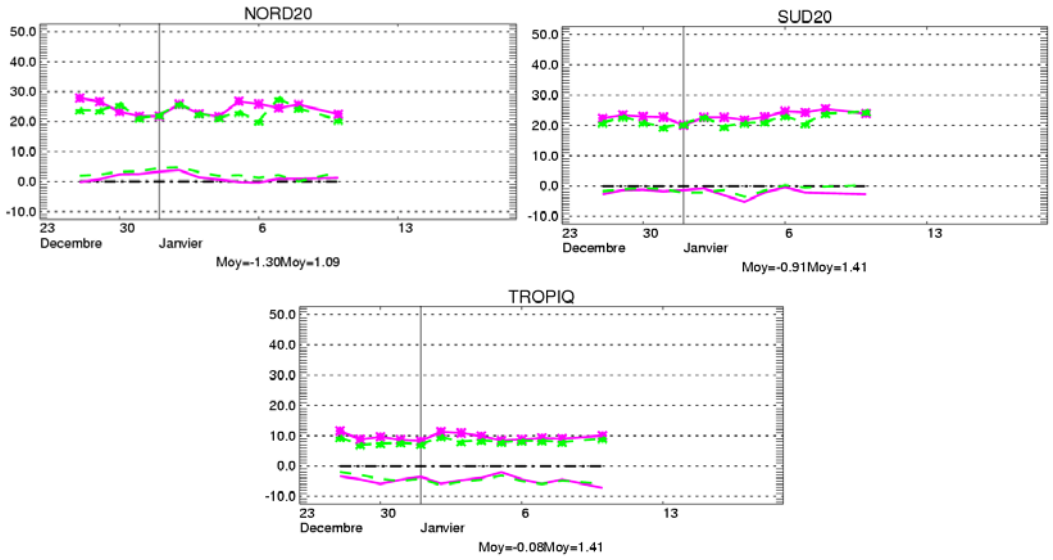

Fig. 6: Time series (winter period) of rms error (curves with symbols) and bias (curves without symbol) for 48 hour forecast of 500 hPa geopotential height when compared to each experiment's own analysis, in the Northern Hemisphere (top left), the Southern Hemisphere (top right) and the Tropics (bottom panel). Control without HIRS data in pink, Experiment with HIRS data in green.

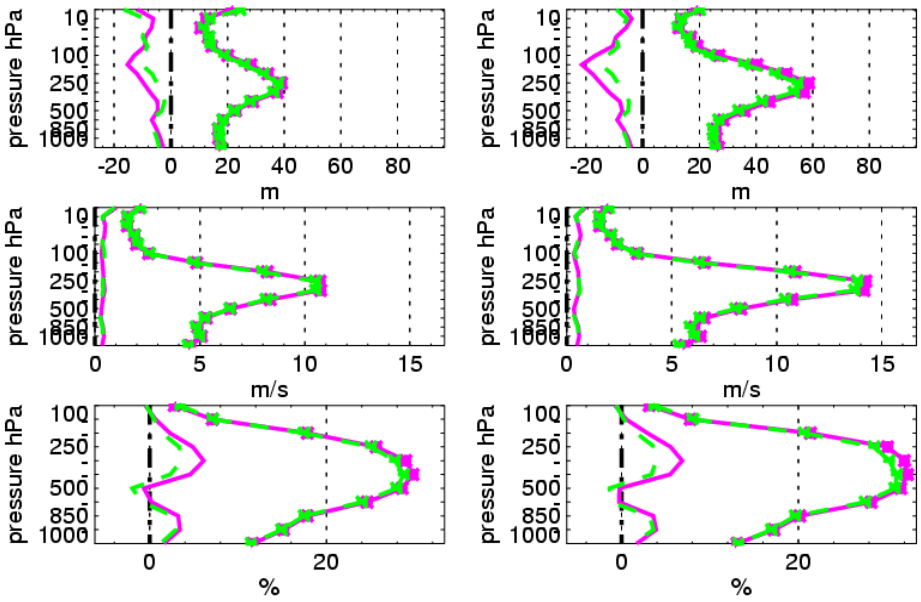

Fig. 7: Profiles of rms error (curves with symbols) and bias (curves without symbol) averaged over the summer period for 72 hour forecast (left panels) and 96 hour forecast (right panels) of geopotential height (top panels), wind (middle panels) and relative humidity (bottom panels). Scores are computed with respect to each experiment's own analysis over Europe and North Atlantic Ocean. Control without HIRS data in pink, Experiment with HIRS data in green.

Assimilation of AMSU B raw radiances

Humidity sensitive microwave channels have the particularity over infrared channels to require less stringent cloud detection. AMSU B has five microwave channels sounding the atmospheric humidity from the lower troposphere to the upper troposphere. However these channels are very sensitive to temperature too. This makes the assimilation of AMSU B data a delicate operation requiring a very good knowledge of the temperature and moisture background error statistics.

Low peaking channels are not used because of uncertainties on the description of the surface properties; only channels 3 to 5 are used, and in the same conditions as at ECMWF, as described in Table 4.

Table 4: Conditions of use of AMSU B channels. Each condition is necessary but not sufficient. T_s is the model surface temperature, obs-fg is the observation departure from first guess, orog stands for altitude and ch for channel. Blue ✓ refers to specific sub-conditions.

Conditions of use ✓	**1**	**2**	**3**	**4**	**5**
9 < scan position < 82			✓	✓	✓
Sea			✓	✓	✓
Land orog < 1000/1500 m for channels 4/5				✓	✓
Ts > 278 K and $\|obs-fg\|_{ch\,2}$ < 5 K			✓	✓	✓

An experiment using AMSU B data (from NOAA16 and NOAA17) on top of AMSUA and HIRS data has been run on a summer period (2-17 Aug 2003). The assimilation of AMSU B data proved on this period to be beneficial to geopotential height forecast, especially in the medium range as it helped to reduce the forecast bias when compared to radiosonde geopotential height by about 5 m at 200 hPa at day 4 in the Northern Hemisphere and about 4 m at 200 hPa at day 3 in the Southern Hemisphere.

As an example of the positive impact of AMSU B data on the forecast performances, Fig. 8 illustrates a comparison of 2 day forecasts at 250 hPa obtained with and without AMSU B data for a perturbation in the North Eastern part of Pacific Ocean. Without AMSU B data the low straddles the ocean and the coast, whereas with AMSU B the low is located over the ocean, at the same place as the Experiment or Control verifying analysis. Moreover the low value in the Experiment forecast (1036.0 dam) is closer to the verifying analysis of the Experiment (1039.6 dam) or Control (1039.7 dam) than the low obtained in the Control forecast (1035.1 dam).

As for temperature and humidity forecast performances, results are more mixed. It is probably too early to draw conclusions from this single 2 week experiment.

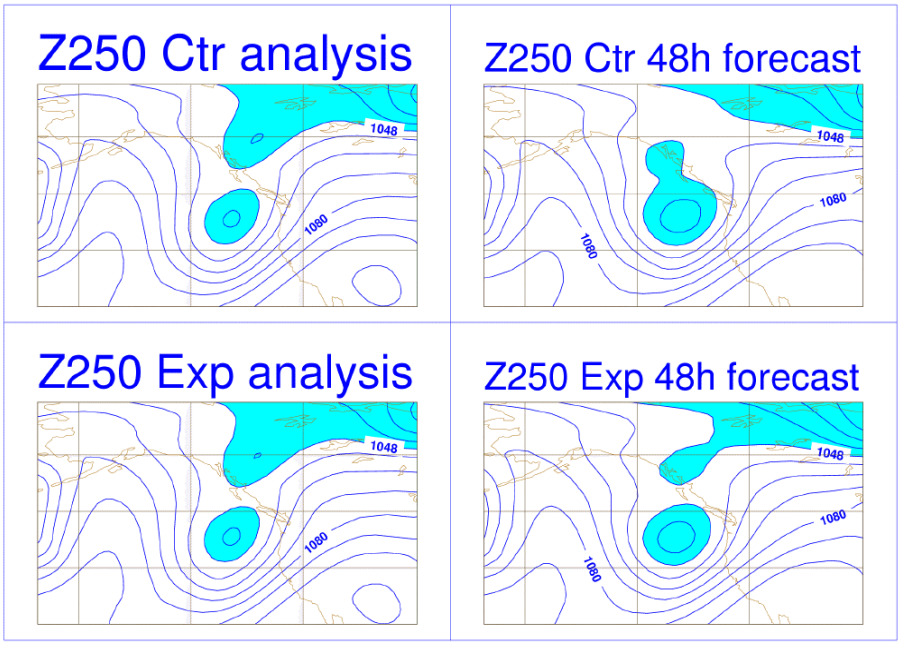

Fig. 8: Maps of 250 hPa altitude (geopotential height divided by gravity constant and by a factor of 10, resulting unit in dam) in the North-East Pacific Ocean. The right panels show the 2 day forecasts verifying 8 Aug 2003 at 00 UTC and the left panels show the verifying analyses. Control (without AMSU B data) charts are on the top, Experiment (with AMSU B data) charts on the bottom. The contour intervals are 8 dam.

Summary and perspectives

The assimilation of each ingredient of ATOVS instrument proved / are expected to be beneficial to the forecast performances of the global model at Météo-France.

(1) Using AMSU A raw radiances instead of AMSU A and HIRS pre-processed radiances improved the short range forecast, particularly in the upper troposphere and in the Southern Hemisphere.

(2) Using HIRS raw radiances in addition to AMSU A raw radiances improves the humidity initial conditions through a global drying of about 4 to 6 %, especially in the Tropics and Southern Hemisphere, and thus reduces the too strong cyclonic activity of the model in the Tropics. Using HIRS data positively affects the geopotential forecast performances below 200 hPa as well as temperature forecast performances, and to a larger extent wind and humidity forecast scores.

(3) Using AMSU B raw radiances in addition to AMSU A and HIRS radiances is expected to improve the medium range forecast performances, but the preliminary results obtained from a single 2 week experiment can not be considered as robust signals.

At the time of the XIIIth TOVS conference, the assimilation of HIRS data was being tested in a pre-operational suite. It became operational on 8 December 2003 with an improved data extraction procedure: instead of a regular sampling of the dataset according to geographical criterion, regular extraction boxes of about 125km×125 km are defined over the globe, in which the HIRS report, which has the largest channel 8 radiance observation value, i.e. the report that has the lowest chance to be cloud contaminated, is selected. This measurement physics-based extraction increases of about 26% the number of HIRS data

used in the assimilation, as the data presented to the assimilation are of better quality and thus less subject to rejection in the first guess quality control.

Experiments with AMSU B data will be run on other periods, with updated bias correction coefficients (as a first approach, bias correction coefficients were computed with respect to the first guess unaware of the existence of AMSU B data, which is the usual preliminary procedure, before any assimilation of new observations).

Optimisation of the use of ATOVS data will then be performed in several directions: revision of data thinning and blacklisting, update of the radiance background error statistics used in the first guess quality control, tuning of the radiance observation error according to the objective method developed at Météo-France (Chapnik et al. 2003).

Another panel of our activities on ATOVS data will be the use of rapidly available EARS (Eumetsat ATOVS Retransmission Service) and Lannion data in the limited area model ALADIN (and later on the mesoscale AROME model to be operational in 2008 at Météo-France), benefiting from the readiness of the 3DVar which will be run in test mode this winter. Impact of those data, of special interest for short cut-off time analysis, will be compared to that of MSG/SEVIRI data (see Montmerle 2003).

References

Chapnik, B., Desroziers, G., Rabier, F. and Talagrand, O. 2003. Estimation of AMSUA radiance error statistics using an optimality criterion. In proceedings of the 13th International TOVS Study Conference (ITSC-XIII), 28 Oct – 4 Nov 2003, Ste Adèle, Canada.

Gérard, É., Rabier, F., Dahoui, M. and Sahlaoui, Z.. 2002. Use of global ATOVS and SSM/I observations at Météo-France. In Proceedings of the 12th International TOVS Study Conference (ITSC-XII), 27 Feb – 5 Mar 2002, The Cumberland, Lorne, Victoria, Australia.

Harris, B. and Kelly, G. 2001. A satellite radiance bias correction scheme for data assimilation. *Quart. J. Roy. Meteor. Soc*., **127**, 1463-1468.

Kelly, G. 2003: Use of satellite radiances in the operational ECMWF system; In proceedings of the 13th International TOVS Study Conference (ITSC-XIII), 28 Oct – 4 Nov 2003, Ste Adèle, Canada.

Montmerle, T. 2003. Impact of the assimilation of MSG/SEVIRI radiances in a mesoscale NWP model. In proceedings of the 13th International TOVS Study Conference (ITSC-XIII), 28 Oct – 4 Nov 2003, Ste Adèle, Canada.

Acknowledgements

We are very grateful to ECMWF for providing the code updates to optimally ingest the ATOVS data within the ARPEGE/IFS collaboration between ECMWF and Météo-France. We also acknowledge the help given by the members of the Satellite Section of ECMWF in providing the blacklist for each instrument of ATOVS and giving an answer to our questions.